This study explores the contact pair «trolleybus contact insert «TCI-power wire». The task addressed relates to the lack of consideration of thermal effects, phase changes, and thermal softening of the material in the classical Archard and Karman models, which complicates wear prediction.

To solve this problem, an energy-temperature wear model (ETW) has been constructed, which integrates mechanical, thermal, and energy processes in the contact zone. Unlike existing approaches, the model considers the temperature-dependent hardness H(T) and local fields of contact pressure and frictional stresses, determined by the finite element method (FEM) in the Ansys environment.

The research features involve a hybrid approach to wear prediction – the integration of mathematical modeling and FEM simulation. The results include von Mises stresses $\sigma_{max} = 16.24$ MPa (amorphous carbon), 18.99 MPa (electrographite – EG), and 30.53 MPa (copper-graphite composite Cu-40%C(f) 0.90 – CU). Under sliding conditions of $S_{total} = 0.2$ m at contact pressure $p = 0.5$ MPa, the wear depth for EG is $1.99 \cdot 10^{-5}$ mm, which is extrapolated to 47.8 mm at 450 km and exceeds the permissible 10 mm, while for CU the wear decreases to 2.2 mm. The wear reduction is associated with the greater hardness of CU (120–135 HV) and a uniform distribution of contact stresses, which confirms the ETW effectiveness.

Practical significance of the results is the possibility of a reasonable choice of TCI materials, in particular copper-fullerene composites (Cu-0.5% FS), to increase wear resistance and stability of current collection with priority insert wear over the contact wire. The scope of practical implementation of the results includes the design of materials for current collection systems of electric transport

Keywords: frictional interaction, fullerene soot, contact insert, wear prediction, energy model

UDC 629.113
DOI: 10.15587/1729-4061.2026.354922

WEAR PREDICTION AND MATERIAL SELECTION OF CONTACT INSERTS FOR ELECTRIC TRANSPORT BASED ON ENERGY MODEL USING THE FINITE ELEMENT METHOD

Kostiantyn Holenko
PhD, Senior Lecturer*
ORCID: https://orcid.org/0000-0002-6140-4573
Oleksandr Dykha
Corresponding author
Doctor of Technical Sciences, Professor, Head of Department*
E-mail: tribosenator@gmail.com
ORCID: https://orcid.org/0000-0003-3020-9625
Orest Horbay
Doctor of Technical Sciences, Professor
Department of Design Machine and Automotive Engineering
Lviv Polytechnic National University
Bandery str., 12, Lviv, Ukraine, 79013
ORCID: https://orcid.org/0000-0002-0915-5637
Oleksii Kovtun
PhD Student*
ORCID: https://orcid.org/0009-0000-6036-6723
Volodymyr Dytyniuk
Doctor of Philosophy (PhD), Lecturer*
ORCID: https://orcid.org/0000-0001-6377-524X
*Department of Tribology, Automobiles and Materials Science
Khmelnytskyi National University
Institutska str., 11, Khmelnitsky, Ukraine, 29016

Received 11.12.2025
Received in revised form 05.03.2026
Accepted 16.03.2026
Published 30.04.2026

How to Cite: *Holenko, K., Dykha, O., Horbay, O., Kovtun, O., Dytyniuk, V. (2026). Wear prediction and material selection of contact inserts for electric transport based on energy model using the finite element method. Eastern-European Journal of Enterprise Technologies, 2 (7 (140)), 44–61. https://doi.org/10.15587/1729-4061.2026.354922*

1. Introduction

The issue of trolleybus contact inserts (TCIs) wear is one of the key factors in the reliability and energy efficiency of urban electric transport systems. It is the TCI that forms direct frictional contact with the contact wire, enabling stable current collection, minimal energy losses, as well as maintaining the integrity of the contact network. Unlike the wire, which is an element of expensive and complex infrastructure, the insert belongs to the replaceable operational components, the wear of which must be a priority, that is, controlled and predicted before the wire is damaged. This condition determines the basic criterion for the safety and economic feasibility of the entire power supply system.

Enhanced requirements for the safety and durability of transport electrical systems in accordance with numerous regulations by the United Nations Economic Commission for Europe (UNECE) stimulates the advancement of certification studies. For example, the R100 Regulations establish permissible levels of mechanical loads and accelerations for electric vehicles. Within these norms, maximum lateral accelerations (up to 10 g) create additional dynamic pressures of the CCT on the wire during turns and oscillations of the current collector rods, which intensifies local processes of friction, heat generation, and wear of the insert mate-

Copyright © 2026, Authors. This is an open access article under the Creative Commons CC BY license

rial. For this reason, the assessment of wear only taking into account normal pressing is no longer sufficient – an energy-temperature assessment is required, covering real operating conditions, including transverse loads and temperature peaks.

It is known that more than 60% of friction losses in current collection units are associated with non-stationary contact modes, when the distributions of pressure, temperature, and sliding speed change over time. Under such conditions, the classical Archard or Karman models are unable to fully take into account thermal softening, phase transitions, or local friction energy, which directly determines the wear rate. Despite the extensive coverage of the tribological behavior of contact inserts in scientific literature, most existing wear models are focused mainly on the mechanical parameters of the contact and do not take into account the complex influence of local heat release and the energy balance of friction. Therefore, there is a need to devise an effective method for quantitative wear prediction that reproduces the complex multifactorial interaction in the contact zone «TCI-wire», reflecting its behavior under real loads, consistent with UNECE standards. The multifactorial nature of tribological interaction should be determined by the simultaneous influence of mechanical, thermal, and energy processes in the contact zone.

Thus, the relevance of our research is due to the need to increase the durability of the contact pair «TCI-wire» and ensure the reliability of current collection under conditions of intensive operation of electric vehicles. Special attention should be paid to devising such approaches to the assessment of friction and wear processes that could take into account the complex influence of mechanical, thermal, and energy factors in the contact zone.

2. Literature review and problem statement

Considering that TCI is only one of the elements in the trolleybus power supply system, it is advisable to investigate its other components and the corresponding electromechanical interconnections. The research results in the following papers report the modeling and optimization of electromechanical and energy processes in trolleybus systems and their infrastructure, focusing on energy consumption, power management, and network integration.

The processing and analysis of data recorded by the trolleybus data acquisition system using LINQ (Language Integrated Query) technology are described in work [1]. The data acquisition system records a large amount of electromechanical information in real time, which is subsequently analyzed to assess the technical condition of the trolleybus batteries. The authors of study [2] proposed a new approach to modeling electric transport, which takes into account both mechanical dynamics and power supply losses and subsystem interaction, which correlates with the problems of current research. This allowed them to reproduce, for example, the effect of voltage drops on acceleration or regenerative braking energy losses due to a temporary lack of network capacity, which also depends on TCI. The method was tested on the trolleybus system in Pilsen (Pilsen, Czech Republic) where the difference between the model and measurements did not exceed 5%, which indicates the high efficiency of the applied analytical approach to full-scale simulation.

In [3], the electromechanical system of the 8000 series trolleybuses in the city of Athens was analyzed based on data from OSY S.A. (Road Transport S.A.). Modeling was carried out to assess energy consumption and energy saving potential due to regenerative braking, the operation of an asynchronous motor and its control schemes (DVC (direct vector control) and DTC (direct torque control) were considered. Additionally, the developers proposed a hybrid energy storage unit to support the efficient operation of the trolleybus VCT, which is the subject of research.

Paper [4] considers the development of trolleybus energy networks as elements of "smart cities". The work models the electrical infrastructure of trolleybuses (using the example of Bologna) in MATLAB-Simulink to assess its integration with renewable sources, energy storage systems and charging stations, which contributes to the decarbonization of urban transport. The authors analyze only the electrical energy efficiency and network integration of trolleybus systems but do not consider tribological processes, where energy losses occur due to friction, heat, and wear.

Work [5] reports construction of a model of a trolleybus network to analyze the energy consumption of innovative trolleybuses with recharging while driving (IMC – in-motion charging). The model is built on the basis of real voltage and current measurements of the Bologna traction substation, which makes it possible to reproduce the change in the number of vehicles during the day and simulate energy processes with high accuracy.

The above studies [1–5] show that increasing the energy efficiency and reliability of trolleybus systems is achieved by improving the models of electromechanical dynamics, traction drive control, regenerative braking, and optimization of power grid parameters. However, issues related to the influence of tribological contact interaction in the pair "VCT-contact wire" on the energy balance and durability of current collector elements remain unresolved. In particular, there are no models that would quantitatively describe the conversion of friction energy into wear of the insert material. The reason for this may be the priorities of the modern electric transport market, formed under conditions of extremely high global competition between manufacturers and city operators. Under such conditions, the key attention is on macro-level tasks, in particular, network optimization, increasing energy efficiency and reducing operating costs. In contrast, micro-level issues related to the study of the efficiency of current collector elements in contact with the wire often remain outside the focus of systemic research.

For the above reasons, papers with an emphasis on contact problems were analyzed. This approach was used in [6], in which a factor analysis of the operational parameters of the steel-aluminum contact in the city's trolleybus network was conducted. The influence of the pressure in the contact pair, the road slope, and the current strength on the wear of the wire was studied, and it was shown that it is the electrical load that has the greatest destructive effect. As a result, the use of a new wire in areas with low traffic and low currents was recommended, but the possibility of selecting alternative TCI materials was not considered.

The authors of study [7] analyzed the relationships in the contact zone "contact wire-current collector insert", comparing the quality and properties of inserts by different manufacturers. The dependence between the hardness and electrical resistance of the material was revealed, and it was proposed to narrow the permissible hardness range and a

method of sorting carbon inserts by structural parameters, which allows reducing the wear of the contact pair. Within the framework of the ACTCCS (Active Control of Trolleybus Current Collection Systems) project [8], a dynamic model of the trolleybus-catenary system was built, taking into account the pre-pressing and self-generated contact force. Their interdependence and role in stable current collection without sparking or loss of contact were studied. Simulations showed that without self-generated force, the system does not provide reliable contact, which is important for all types of pantographs (including railway ones). It should be noted that the model considers only the mechanical interaction and force dynamics (without assessing the energy or thermal load on the wire). Heating from the current, friction coefficient, dissipation energy, or local temperature peaks (flash temperature) are not taken into account. On the other hand, the problems described in the paper are correlated with the task of determining the pressure of the contact wire on the contact wire, which is modeled in the current study.

In [9], the method of testing and predicting the wear of a sliding contact is substantiated by comparing the calculated results with experimental data. In [10], an experimental study of the tribological characteristics of the contact "copper-silver wire – pure carbon insert" at currents of 300–500 A and speeds of 150–250 km/h is described. The change in the friction coefficient (0.20–0.28) and the wear rate of the inserts are determined, and the main wear mechanisms are established: abrasive, adhesive, layered, and arc. The study provides only experimental data from the macro level, without FEA analysis of the distribution of contact pressure, temperature, and local wear, which is a certain limitation in terms of analytical reproducibility of the results. In [11], a new design of a rotating conductive connection with roller elements is presented, where tribological and electroconductive properties at currents of 0–20 A are investigated. It was found that with increasing current, the friction coefficient and wear intensity increase, and a conflict is observed on the contact surface between hardening due to conductive friction and softening due to the electroplastic effect.

The results from studies [6–11] cover factorial analysis of wear, dynamic modeling of contact, experimental determination of tribological characteristics, and prediction of durability of current collection systems, which is close to the tasks of the current work. Many authors have shown that the electrical load, contact force, hardness of materials, and current collection modes significantly affect the friction coefficient, wear intensity, and contact stability. However, issues related to the consideration of local energy and temperature balance, FEA-distribution of stresses and temperatures, and analytical description of the conversion of friction energy into wear remained unresolved. At the same time, thermomechanical approaches are mostly reduced to the estimation of temperatures/stresses without a direct connection with the wear law, while energy models of wear often do not contain a local FEM-description of the contact state.

In particular, most existing approaches lack integration of thermomechanical analysis with numerical modeling of the local contact state, which limits the possibilities of quantitative prediction of wear in variable current collection modes. The reason for this may be the methodological limitations of existing approaches, focused mainly on experimental or macromodels without integration of thermomechanical analysis of the contact pair. An additional reason is the lack of correlation of the modeled boundary conditions with those specified in accordance with a number of requirements by the UNECE (United Nations Economic Commission for Europe) certification rules. For example, the magnitude of the TCI pressure on the wire and the generated friction stresses are significantly affected by the lateral accelerations of the trolleybus during its motion dynamics. In this context, it is advisable to familiarize yourself with a study [12] on the requirements of the UNECE R100 rules, which regulate the preservation of electrical power elements at regulatory accelerations. According to the R100 testing regulations for a 12-meter low-floor bus or trolleybus, the values should be 12g in the longitudinal direction and 10g in the transverse direction. Thus, the cited paper can serve as a guideline for the formation of boundary conditions for critical loading modes "TCI-wire" within the framework of UNECE regulatory requirements.

A possible solution to the issue of TCI wear may be targeted research and implementation of alternative materials and compositions with controlled conductive, tribological, and thermal properties. In particular, the use of composites or functional coatings capable of providing an optimal combination of hardness, electrical conductivity, and stability of frictional characteristics under conditions of high currents and variable contact loads is promising. Considering that a significant part of current research reports the comparative analysis of different TCI materials in contact with a power wire, it is worth familiarizing yourself with modern works in the field of electrical materials science.

In [13], the mechanical and tribological properties of electrodeposited Ag/graphene coatings for electric vehicle charging contacts under conditions of sliding friction and conductive fretting were investigated. The authors showed an increase in hardness, a decrease in the coefficient of friction and wear, as well as the formation of a transfer film as the main factor in improving operational characteristics. Work [14] gives a review of modern research on friction and wear of conductive pairs under difficult conditions (aviation, railway transport, armament). The classification of types of conductive wear, factors affecting friction, mechanisms of arc formation, coating degradation and environmental influence are summarized. The technologies for manufacturing conductive self-lubricating materials and methods for predicting the temperature field and the amount of wear are considered.

However, in [13, 14], the issues of quantitative justification of the choice of alternative TCI materials taking into account the local distribution of contact pressure, temperature and friction energy remained unresolved. The relationship between the structural parameters of the material, its hardness, electrical conductivity, and dynamic energy balance in the contact zone has not been sufficiently studied. There is also no integrated methodology that would combine experimental data with FEA analysis and make it possible to assess the local energy balance of friction as a determining factor of wear.

The most promising option for overcoming the difficulties associated with the wear of the current collector inserts when in contact with the power system wire may be the use of modern nanocomposites, for example, Cu-0.5% Fullerene Soot (hereinafter, FS). FS is a representative of a relatively new class of copper-based nanocomposites and is a copper matrix to which 0.5 wt. % fullerene soot is introduced.

Available works focused on studying the features of the integration of fullerenes into the composite base were con-

sidered. The authors of paper [15] investigated the effect of adding fullerenes on the mechanical properties of carbon-epoxy composites (CFRP). The introduction of 0.1–1% fullerenes increased the tensile and compressive strength by 2–12% and increased the interlayer crack resistance by approximately 60%, which is associated with an increase in the deformation capacity of the epoxy matrix. In [16], a metal-impregnated carbon-fiber carbon composite (C/C) was analyzed. It is considered a promising material for contact inserts of pantographs of high-speed electric transport due to its significantly higher bending and impact strength compared to traditional metal-impregnated carbon. It was experimentally established that due to the anisotropy caused by the orientation of the carbon fabric layers, the wear intensity when sliding parallel to the layers is higher than when sliding perpendicular to them, especially at high current densities and frequent arc discharges. This approach is used in current studies when analyzing the Electrographite (parallel to grain) material for CGT, which is fully consistent with the authors of [16].

In [17], a number of commercial carbon nanomaterials were characterized: carbon black with fullerenes, pure C60-fullerene and mixed fullerene material using FESEM (field emission scanning electron microscope). The authors also investigated HRTEM (high-resolution transmission electron microscope), EDS (energy dispersive X-ray spectrometry) and XRD (X-ray diffraction). It was found that carbon black contains a mixture of fullerene and amorphous carbons, pure C60 has a cubic structure, and mixed fullerene includes nanotubes and a small amount of amorphous carbon. Wear in the sliding contact "contact wire-current collector" is determined by the joint action of friction and electrical phenomena (sparking, arc discharges), which are closely and nonlinearly interconnected; therefore, the results of laboratory tests require correct extrapolation to real operating conditions.

In [18], a combined methodology was proposed that combines a wear-map-based wear model with consideration of electric current and numerical simulation of the dynamic interaction of the pantograph with the contact network using instantaneous values of contact forces and currents. The possibility of comparative assessment of wear for copper and graphite contact inserts on DC lines was shown, as well as prediction of the influence of mechanical tension of the contact wire on the level of wear. This correlates with the boundary conditions of current research in the form of pressure from the side of the power network wire on the surface of the TCI trough.

In [19], methods for fabricating metal nanocomposites reinforced with carbon nanomaterials are summarized, with special attention to fullerenes as a promising alternative to nanotubes and graphene. Their advantages are explained: low cost, high purity, resistance to mechanical damage, and the ability to reduce friction due to the spherical shape and strong intermolecular bonds. The work emphasizes the potential of fullerenes as a reinforcing and lubricating phase for tribological applications. In [20], the friction and wear of a carbon-graphite material under high-speed sliding (up to 75 m/s) with and without the flow of electric current were investigated using a specialized test rig. It is shown that the load, sliding speed and electric current significantly affect the tribological behavior of the material, and the presence of current leads to significantly different mechanisms of friction and wear, which is confirmed by the analysis of wear products by the SEM (Scanning Electron Microscopy) method. It is this approach (establishing boundary conditions in the form of displacement over time) that was used by the authors of the current studies – the TCI slides on the surface of a current-carrying wire.

In paper [21], composites based on aluminum oxide reinforced with fullerene carbon black, obtained by mechanical alloying, ultrasonic treatment and spark plasma sintering (SPS), were investigated. The addition of 2% Ni contributes to the transformation of carbon black into nanostructures of diamond, fullerite and graphite, which increases the crack resistance to 16.5 $MPa \cdot m^{1/2}$ and reduces the electrical resistance by 15 orders of magnitude. The strengthening is associated with the formation of a homogeneous carbon coating on Al_2O_3 particles. To analyze the strength of such coatings, a method and its theoretical justification were proposed by the authors of study [22].

In summary, the results of studies [15–22] include the analysis of the mechanical and tribological properties of nanocomposites modified with fullerenes, as well as experimental approaches to assessing their behavior in the presence of electric current. Their authors showed that the introduction of fullerene nanostructures could increase the strength, crack resistance, electrical conductivity, and potentially reduce the friction coefficient due to the structural and molecular features of the carbon phase. However, the issues related to the practical verification of the operation of such materials directly in the contact pair "TCI-wire" under real electrothermomechanical loads remained unresolved. In particular, it has not been sufficiently studied how local contact stresses, temperature gradients, and friction energy affect the wear of such materials under real current collection modes. The reason for this may be the difficulty of reproducing the operating conditions of current collection and the predominant orientation of existing works on materials science analysis without integration with applied tribological models.

Taking into account the above, an option to overcome the difficulties of quantitative assessment of the efficiency of fullerene composites may be the use of FEA simulation in the Ansys environment or alternative ones. This approach makes it possible to integrate electrical, thermal, and mechanical loads within a single calculation model and reproduce actual boundary conditions of current collection. The authors of [23, 24] built a multifactor model of electromechanical processing (EMP), which combines thermal and mechanical loads on the surface layer of the material. Based on the model in Ansys Static Structural and Coupled Field, an approach was devised that provides a physically justified description of the interaction of current, heat, and mechanical pressure in the contact zone.

From the point of view of the current research topic of the contact pair "TCI-wire", this work is a methodological guide to the formation of boundary conditions in the Ansys Coupled Field environment. The EMP model describes similar physical processes of local heating, electroplasticity, and surface stress that occur during current collection. Thus, the results of EMP simulation lay a scientific basis for interpreting thermomechanical effects in the "TCI-wire" contact, in particular, the formation of surface hardening zones, temperature gradients, and hardness changes that determine the real wear mechanism.

Our review of the literature [1–24] revealed that available studies cover individual aspects in the functioning of trolleybus power supply systems – from the analysis of energy flows and modeling of network processes to the materials

science and tribological characteristics of the elements of the contact pair. At the same time, it was found that most current approaches consider mechanical, thermal, and energy processes in the "insert-wire" contact zone mainly in isolation, without their complex combination under actual operating conditions. Available scientific publications do not sufficiently cover the issue of integrating thermomechanical FEA analysis of the contact state with the energy description of the wear process. Most studies are either focused on the macro level (energy and network processes) or the micro level (structure and properties of materials), while the critical intermediate level (local energy-temperature and mechanical interaction in the contact zone) remains insufficiently studied.

The above allowed us to state that it is advisable to conduct a study on the wear of the contact pair "insert-wire" based on an integrated energy approach taking into account temperature effects and numerical modeling of contact interaction.

3. The aim and objectives of the study

The purpose of our study is to predict the wear of the contact pair "TCI-power wire" and select materials based on the energy model using the finite element method to reproduce real contact pressure fields and frictional stresses in the interaction zone. The desired result is to verify the priority of wear of the contact insert compared to the wire, to quantitatively assess the influence of thermomechanical parameters on the intensity of wear, and to justify the choice of TCI materials with increased wear resistance.

To achieve the goal, the following tasks were set:

– to construct and implement an energy-temperature model of wear taking into account local contact pressure fields $p(x,y,t)$ and frictional stresses $\tau(x,y,t)$, to compare it with existing classical Archard and Karman models, and to quantitatively determine the wear of TCI;

– to perform numerical simulation of the contact interaction within the "TCI-wire" pair in the Ansys environment and, based on the energy model, evaluate the wear of TCI materials, comparing the obtained values with the regulatory limits, and determine the prospects for copper-fullerene composites Cu-0.5% FS.

4. The study materials and methods

4. 1. The object and hypothesis of the study

The object of our study is the contact pair «trolleybus contact insert (TCI) – contact wire», which provides current collection in the trolleybus power supply system.

The principal hypothesis assumes the determining role of the combined action of mechanical, thermal, and energy factors in the contact zone «TCI-wire», which necessitates their integrated energy-temperature consideration when predicting the intensity of wear.

The assumptions adopted:

– the contact between the trolleybus contact insert and the contact wire were considered as a localized zone of sliding frictional interaction;

– the main factors determining the intensity of wear were taken to be contact pressure, sliding speed, temperature, and local friction energy;

– heat generation in the contact zone was determined by the dissipation of friction energy;

– mechanical and thermal processes in the contact zone were considered to be interconnected.

The accepted simplifications:

– the geometry of the contact system is represented in the form of a localized calculation area, which reproduces the characteristic section of the "TCI-wire" interaction;

– the wear of the contact wire within the model was not considered as a determining factor and was taken into account indirectly through the condition of priority wear of the insert;

– the calculation was performed for characteristic load modes without reproducing the full spectrum of random operational disturbances;

– the model took into account mechanical and thermal processes of the contact without taking into account chemical and electrical-erosion effects.

4. 2. Wear models and formulation of the energy-temperature model of insert wear

Before conducting FEA wear analysis, it is critically important to consider existing analytical and semi-empirical models of wear prediction as they specify physically based relationships between load, material properties, and friction energy. This allows us to correctly select parameters for numerical simulation, avoid incorrect interpretation of results, and ensure consistency between theoretical assumptions and numerical calculations:

1. Archard model. The Archard wear model, due to its relative simplicity, is widely used for modeling abrasive and adhesive wear, especially in mechanical systems with body contact. The classical equation of the model is

$$V = \frac{K \cdot F \cdot s}{H}, \tag{1}$$

where V is the wear volume, m^3; K is the wear coefficient (dimensionless quantity); F is the load, N; s is the sliding length, m; H is the material hardness, Pa. The wear coefficient K (Wear Coefficient) depends on the material pair, lubrication conditions, etc. (typical values: $10^{-3}...10^{-6}$). Example: if $K = 10^{-4}$, $F = 1000$ N, $s = 10$ m, $H = 1 \cdot 10^{19}$ Pa, then $V = 1$ mm^3.

The Archard model can be written in terms of the integral over the contact area. If there is a contact field of distributed pressure $p(x,y)$ and a known coordinate-dependent sliding function $s(x,y)$, the value of V can be calculated as follows

$$V = \iint_A \frac{K \cdot p(x,y) \cdot s(x,y)}{H} \mathrm{d}A. \tag{2}$$

Since the force F is the integral of the local pressure $F = \iint p(x,y)\mathrm{d}x\mathrm{d}y$, from equation (1) we can determine the local wear depth $d(x,y)$ through the following transformations:

$$d(x,y) \cdot A(x,y) = K \cdot \frac{p(x,y) \cdot A(x,y) \cdot s(x,y)}{H},$$

or

$$d(x,y) = K \cdot \frac{p(x,y) \cdot s(x,y)}{H}, \tag{3}$$

where $p(x, y)$ is the local pressure, Pa; $s(x, y)$ is the local sliding length, m; $A(x, y)$ is the elementary area of the contact area (the area of a finite element or nodal region on the contact surface), m^2.

For the total wear volume

$$V_{total} = \iint_A d(x,y)\mathrm{d}A = \sum d_i \cdot A_i, \quad (4)$$

where A_i is the area of the element/nodal region, m^2.

Literary notation of the equation of the Archard model is

$$W = \frac{\Delta m}{L \cdot \rho \cdot F}, \quad (5)$$

where W is the wear in the form of specific wear, mm^3/(N·m); Δm is mass loss, g; ρ is density, g/mm^3, N; L is sliding length, m.

Equation (5) is used in experimental conditions, when mass loss is fixed and wear is calculated in terms of force and path. It describes the real measured wear volume.

Relationship between the experimental wear equation (measured mass) (5) and the classical Archard equation for numbers or FEM (1). If we multiply both sides of equation (5) by $F \cdot L$ and take into account that $V = \Delta m / \rho$ (wear volume), then $W \cdot F \cdot L = V$, which is already similar to the classical model (1), so the relationship between the equations is as follows: $K = W \cdot H$. The unit of measurement W means how many mm^3 of material is worn when a force of 1 N is applied over a sliding distance of 1 m.

Disadvantages of the Archard model: it ignores the effect of temperature and thermal softening of the material; it does not take into account the change in the coefficient of friction or the appearance of protective films; it considers hardness as a constant value, which is incorrect during dynamic heating.

2. The Karman model (Khruschov, Rabinowicz, Holm-Archard extended) takes into account the properties of the material in more detail and is an extended Archard model. This is an energy approach to modeling wear, which refines the classical Archard model by taking into account the dissipation of friction energy. The idea of the Karman model (and its extensions): material wear is considered as the result of the conversion of part of the mechanical friction energy in the sliding process into plastic deformation and separation of particles (that is, wear). Unlike the simple Archard model, here not only hardness and contact force are important but also the real work of friction

$$\Delta V = \eta \cdot \frac{\mu \cdot F_N \cdot s}{H}, \quad (6)$$

where μ is the friction coefficient; F_N is the normal load, N; η is the wear coefficient, which is responsible for the fraction of energy that is actually spent on wear (the rest is dissipated in the form of heat, vibrations, elastic deformations, etc.). Typical values: 0.001–0.1 for dry friction; less than 0.001 – for lubrication or very hard materials.

Historically, the evolution of models consisted of the following stages: the Holm model (1909), in which wear was first associated with pressure and displacement; the simplified Archard model (1953) based on hardness assessment; the Khruschov/Rabinowicz model (1950–60s) with an energy interpretation (wear depends on the work of the friction force). Finally, the Karman model expanded the wear theory and introduced the concept of the surface destruction efficiency coefficient (η), thereby generalizing previous models.

Disadvantages of the Karman model: the efficiency coefficient η is considered constant or slightly variable; the dependence on the sliding speed and on the local thermal regime is not taken into account; phase transitions or surface degradation due to overheating are ignored.

3. Energy models consider wear as the result of the expenditure of part of the mechanical friction energy on plastic deformation and separation of particles from the contact surface. General equation is

$$V = \alpha \cdot E_{frict} = \alpha \cdot \int p \cdot \Delta u \mathrm{d}A, \quad (7)$$

where α is the global efficiency coefficient of energy conversion into wear, mm^3/J; E_{frict} is the friction energy (total or local), J; p is the contact pressure or normal force per area, Pa; Δu is the relative shear displacement, m; dA is the contact area element, m^2.

Simplified local wear formula (depth) is

$$d(x,y) = \frac{\eta \cdot \tau(x,y) \cdot s(x,y)}{H}, \quad (8)$$

where η is the local efficiency coefficient of energy conversion into wear; τ is the tangential stress (Frictional stress), Pa.

Format for applied calculation based on FEA results Ansys (or alternative processor) is

$$d = \frac{\eta \cdot \tau_{avg} \cdot S_{total}}{H}, \quad (9)$$

where τ_{avg} is the average value of Frictional Stress from Ansys, Pa; S_{total} is the total sliding distance measured in Ansys, m.

Among the above models, the most accurate is considered to be the energy model, in particular, its local analytical form (8) for mathematical prediction, and the post-processing form (9) for verification FEA calculations. Due to the high level of applicability of the energy model, it was chosen to process the results of FEA simulation wear, given below.

4. For full coverage of the topic of analytical analysis of wear, it is advisable to provide other existing models. The Freudenthal-Cogan model uses the concept of damage accumulation in the material due to plastic deformation, and wear is associated with plastic shear and the critical volume of the plastic zone. The Lancaster wear law relates the wear rate to the specific frictional energy per unit mass of material lost. Tribo-oxidation models take into account the formation and destruction of the oxide film (real surfaces often wear not only due to the abrasive-adhesive mechanism, but also due to chemical reactions in the contact zone). Fretting fatigue / fatigue wear models are based on the cyclic accumulation of damage, when even with small sliding displacements microcracks accumulate, leading to delamination of particles. Holm-Perry scaling models use the scaling of the size of contact spots and the microtopography of surfaces. Models based on the theory of linear damage (Miner's rule adaptation) consider wear as the equivalent of accumulated "damage work", similar to the fatigue approach.

5. Tribology is increasingly gaining ground in the list of areas of energy conservation research, as reducing friction costs is literally dictated by market competition among manufacturers. Increasing the efficiency of any component or unit or system can no longer be achieved by just a few design or technological measures, as it was 50–70 years ago in the

era of the rapid development of the automotive industry. Each (even the smallest) step towards minimizing energy losses has weight and forms the overall economy of the system as part of numerous optimization measures.

Taking into account the rapid evolution of tribology and the analysis of existing wear models, we have proposed a new hybrid model of Energy-Temperature Wear (ETW). Its purpose is to take into account not only the mechanical work of friction but also the local heat balance in the contact zone. The idea of the model: wear is proportional to the effective friction energy that cannot be dissipated by the material as heat or reversible deformations. The energy is converted into irreversible damage to the surface (e.g., through thermal conductivity, elastic vibrations, acoustic radiation, or other reversible processes). Formalization of the determination of the wear volume is

$$V = \int_A \eta\left(T,p,s'\right)\frac{\tau \cdot s}{H\left(T\right)}\mathrm{d}A, \tag{10}$$

where $\eta(T,p,s')$ is the local efficiency coefficient of energy conversion into wear (dimensionless), which depends on temperature, pressure and sliding speed; $\tau \cdot s$ is the friction work per unit area, J/m^2; p is the normal contact pressure, Pa; $H(T)$ is the temperature-dependent hardness (taking into account the thermal softening of the material), Pa; T is the local temperature, K; dA is the contact area element, m^2.

The selection of ETW model parameters (except for those directly determined by the results from FEA analysis) is usually performed on the basis of laboratory studies in materials science and engineering centers at manufacturers of urban electric transport. These parameters are formed by matching the calculated wear dependences with known experimental patterns for contact pairs of the "carbon material-copper wire" type. This approach provides a physically justified parameterization of the model during its predictive application for wear assessment.

ETW innovation: nonlinear relationship between temperature and hardness; phase transformations (e.g., oxide film formation); possibility of combining mechanical, thermal, and chemical mechanisms in one formalism.

The proposed ETW model is focused on the analysis of sliding contact in current-carrying units of electric transport and is intended for comparative evaluation of contact insert materials under given load conditions. At the same time, the model does not take into account stochastic effects of sparking, degradation of the contact surface, and long-term electrochemical processes, which determines the limits of its application.

The transition from the general idea (10) to the applied algorithm for Ansys (or alternative processors) is as follows:

1. Model kernel with dimensionalities. The proposed local wear rate (wear depth increase per unit time) at point (x, y) and its time-integrated form t can be written as

$$d'\left(x,y,t\right) = \frac{\eta\left(T,p,v\right)\cdot\tau\left(x,y,t\right)\cdot v\left(x,y,t\right)}{H\left(T\left(x,y,t\right)\right)},$$

$$d\left(x,y\right) = \int_0^{t_f}\frac{\eta\left(T,p,v\right)\tau v}{H\left(T\right)}\mathrm{d}t, \tag{11}$$

where d is the local wear depth, m; $H(T)$ is the hardness taking into account thermal softening, Pa; $\eta(T, p, v)$ is the efficiency of converting friction into material separation (dimensionless); p is the normal contact pressure, Pa; T is the local temperature, K.

2. Connection with data from Ansys (discrete form). Let there be time steps t_n and a grid of contact elements / nodal regions i with area A_i. Discretization:

$$\Delta d_i^{(n)} = \frac{\eta\left(T_i^{(n)},p_i^{(n)},v_i^{(n)}\right)\tau_i^{(n)}v_i^{(n)}}{H\left(T_i^{(n)}\right)}\Delta t^{(n)},$$

$$d_i = \sum_n \Delta d_i^{(n)}, \quad V = \sum_i d_i A_i, \tag{12}$$

where d_i is the local wear depth in the i-th contact area, m; V is the total wear volume (the volume of material lost due to friction), m^3.

Practical Ansys parameters that are required:

– $T_i^{(n)}$ (TEMP) is the temperature;

– $p_i^{(n)}$ (CPRESS) is the contact pressure;

– $\tau_i^{(n)}$ is the modulus of shear / frictional stress in the contact (CSHEAR or equivalent).

The $v_i^{(n)}$ value is taken either directly (RELTANGVEL) or from the time derivative of the tangential slip increment (CUM SLIDING DIST) as $v \approx \Delta s / \Delta t$. A_i is the area of the element (from geometry).

3. Temperature dependence of hardness $H(T)$. At this stage, a material model (from an experiment or a reference book) is required. Possible modeling options:

– linear softening to the tempering temperature

$$H\left(T\right) = H_o\left[1-\beta\left(T-T_0\right)\right], \quad 0 \le \beta\left(T-T_0\right) < 1; \tag{13}$$

– piecewise-linear/exponential:

$$H\left(T\right) = \begin{cases} H_0, & T \le T_1 \\ H_0 e^{-\gamma\left(T-T_1\right)}, & T_1 < T < T_2, \\ H_{\min}, & T \ge T_2, \end{cases} \tag{14}$$

where H_0 is the initial (nominal) hardness at the reference temperature T_0, Pa (hardness is often given in Vickers (HV). To convert to Pa: 1 HV $\approx 9.80665 \cdot 10^6$); β is the linear thermal softening coefficient, K^{-1}; T_1 is the softening onset temperature (associated with the onset of active thermal softening or the onset of oxidation), K; T_2 is the end temperature of the active hardness drop (above which the lower threshold is set), K; γ is the exponential coefficient of hardness decay with temperature, K^{-1}; approximately $\gamma = 10^{-3}$–10^{-2} K^{-1} (depending on the material); $H_{\min}$ is the minimum permissible hardness at high T, Pa.

4. Efficiency $\eta(T,p,v)$ and structured calibration. The coefficient η collects the fraction of the friction power that goes specifically to the formation and separation of particles. The basic form for calibration is

$$\eta\left(T,p,v\right) = \eta_0 \cdot f_T\left(T\right)\cdot f_p\left(\frac{p}{H\left(T\right)}\right)\cdot f_v\left(v\right), \tag{15}$$

where all factors are dimensionless, bounded by the upper value (for example, ≤ 1). The function $f_T(T)$ is responsible for thermal effects; $fp(p/H(T))$ is responsible for the degree of plasticity; $fv(v)$ is responsible for the kinematics and film formation.

5. Formalization of equations for use in postprocessing:
– through the friction intensity $qf = \tau \cdot v$

$$\Delta d = \eta\left(T, p, v\right)\frac{q_f}{H\left(T\right)}\Delta t; \quad (16)$$

– through the increment of friction energy on area $\Delta wf = \tau \cdot \Delta s$, J/m^2

$$\Delta d = \eta\left(T, p, \_\right)\frac{\Delta w_f}{H\left(T\right)}. \quad (17)$$

In (17), the parameter _ means that in this form the slip velocity *s'* is not used explicitly because the transition from $\tau v \Delta t$ to the integrated slip increment Δs has already been made.

4. 3. Modeling of the "insert-wire" contact

The object of our research is the trolleybus contact insert (TCI) (Fig. 1, *a*), which is installed in the head of the current collector rod (Fig. 1, *b*) and contacts the transmission wire of the power transmission line (power cable) to connect the current collector to the trolleybus power network. The warranty period of operation of TCI is at least 450 km in dry weather and in the absence of eccentric displacement of the wires at the joints. The depth of the limit wear of the inserts is up to 10 mm.

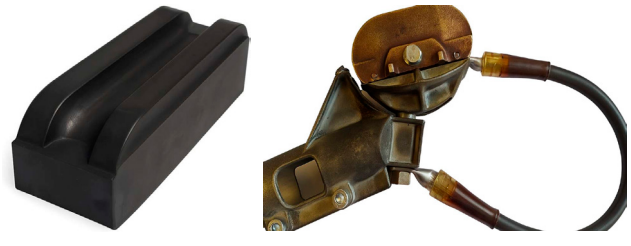

a *b*

Fig. 1. Photographs of the elements in a current collector system: *a* — TCI-4 insert; *b* — rod head

Marking of copper wire MF-100: M – current-carrying multi-wire conductor made of twisted copper wires; F – shaped; 100 – rated cross-sectional area (mm^2). Changing the value of the applied pressure and geometric parameters of the contact area causes instability of the specific load on the insert, which varies within 0.1–0.5 MPa. This leads to intensification of their wear and an increase in energy losses due to friction. The selection of the range of contact pressure and kinematic parameters of the model was carried out on the basis of the operating characteristics of the current-collecting nodes of trolleybus systems, given in the technical specifications for TCI-4, as well as known empirical operational data, which ensures the physical consistency of the boundary conditions of FEA simulation with real current-collecting modes.

A model of TCI and a wire fragment were built using the extrusion method in the SolidWorks environment and their assembly (Fig. 2, *a*) was exported to Ansys Coupled Field Transient. An FE mesh was generated using Ansys Mesh (Fig. 2, *b*) with the following parameters: Body Sizing = 2.0 mm (maximum size of finite elements); Face Sizing = 1.0 mm (on contact surfaces). Inflaction parameter = 9 for the wire and 5 for the insert on their contact surface (the number of layers of finite elements with the size Face Sizing deep into the body). Statistics: 190842 finite elements are connected by 375525 nodes. The contact area of the model is discretized with elements of the Tet10 type (tetrahedron) with local mesh refinement in the contact zone "TCI-wire" (contact refinement). This ensures correct reproduction of contact pressure gradients and friction stresses. The mesh is characterized by an average Jacobian ratio of 0.97, an average skewness of 0.28, and an average aspect ratio of 6.7, which confirms the proper geometric quality of the elements and the numerical stability of the calculation. Additional mesh detailing in the contact zone (reducing the characteristic element size to 0.8 mm) led to a change in the maximum contact stresses by only ≈ 3–4%, while the calculation time increased several times. This indicates that the solution has reached practical convergence and that further mesh detailing is impractical given the ratio of accuracy to computational costs at this stage of research.

The boundary conditions included predefined constraints and loads on the model to simulate full-scale tests. Fixed Support (cantilever clamping) was applied to the upper part of the wire (tag A – model in Fig. 2, *a*). The Pressure value is 0.5 MPa – tag B on the lower face of the insert to simulate its pressing against the wire. The TCI movement was simulated using Displacement = 200 mm (tag C) in the direction of movement along the wire. To limit the movement of the TCI in the transverse direction, which simulates fixation in the head of the current collector rod, the value of Displacement 2 (tag D) was set to 0 mm. Experiment time = 1 s; the minimum number of substeps of the system state $n = 10$. Frictional contact of the surfaces with a coefficient of 0.13 (Fig. 2, *c*), which corresponds to the technical conditions for the operation of the TCI-4. The model adopts a number of simplifying assumptions: isotropy of materials, constancy of the friction coefficient within the calculation interval, and absence of arc discharges in the contact zone. Such assumptions make it possible to focus the analysis on the thermomechanical component of the wear process.

The adopted contact pressure of 0.5 MPa corresponds to the upper limit of the operational loads of the insert on the contact wire, which are formed by the pressing force of the current collector rod and its dynamic oscillations during the movement of the trolleybus. The sliding displacement of 200 mm per 1 s is used as a representative fragment of the relative movement in the contact zone, while the friction coefficient $\mu = 0.13$ corresponds to typical values for contact pairs "graphite-copper" and "copper-graphite composite-copper", given in tribological studies on current collection systems and is consistent with the technical conditions of operation of TCI-4.

FE analysis was performed for 4 different materials (characteristics according to Ansys Granta EduPack in Table 1) of the TCI in contact with the wire. In order to simplify further representation and ensure ease of handling of materials, their abbreviated designations are introduced in the text:

– Carbon (CY) for amorphous carbon-graphite (Morgan Technical Ceramics CY10), hereinafter CY;

– Electrographite (parallel to plane) for electrographite (grain orientation parallel to the plane), hereinafter EG;

– Cu-40% C(f) 0.90 laminate is copper matrix reinforced with carbon fiber (metal matrix composite, Cu-40% C(f), volume fraction 0.90), hereinafter CU;

– Copper C10100 is copper grade C10100 (electrolytic, hard, ETP), hereinafter CO.

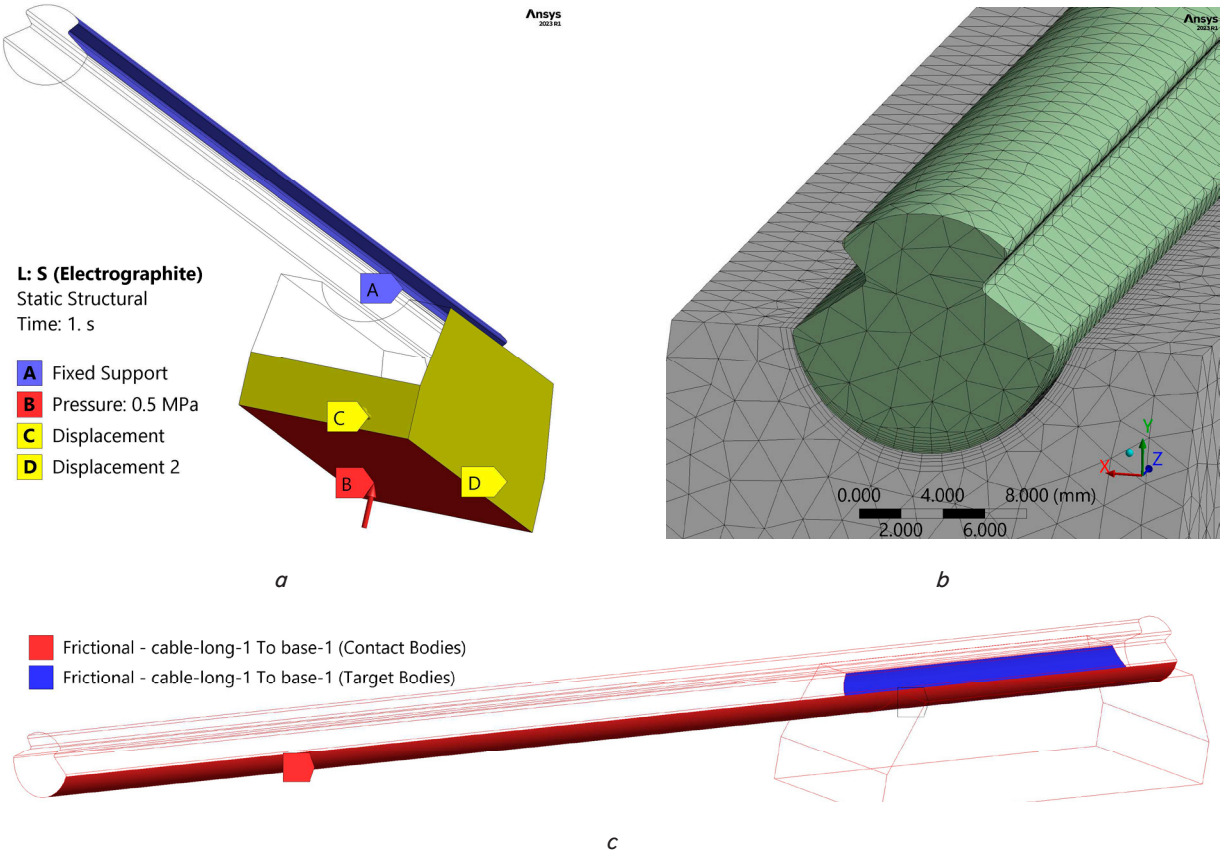

Fig. 2. Ansys model: *a* – boundary conditions (displacement, pressure, and fixation); *b* – finite element mesh of the "insert-wire" assembly model; *c* – frictional contact between the surfaces of the wire and the insert

Table 1

Key material parameters according to Ansys Granta EduPack

Material	Yield strength, MPa	Density $\times 10^3$, kg/m^3	Young's modulus $\times 10^9$, Pa	Shear modulus $\times 10^9$, Pa	Hardness (Vickers), HV	Electrical resistivity, Ohm · m
CY	12.9–14.3	1.58–1.62	9.7–10.3	4.0–4.3	38.7–42.9	$(1.58–5.01) \times 10^{-6}$
EG	1.4–1.6	1.5–1.9	14.6–15.4	6.15–6.45	4.28–4.72	$(6–40) \times 10^{-6}$
CU	400–450	6.06–6.15	143–162	69–79	120–135	$(19.1–20) \times 10^{-9}$
CO	185–340	8.94–8.95	125–135	45–50	80–115	$(17–17.4) \times 10^{-9}$

The purpose of variation of the TCI materials is to determine the optimal contact pair that ensures minimal wear of the insert while maintaining the integrity of the wire surface, which is considered as the basic criterion (axiom) of the study.

5. Results investigating a contact in the "insert-wire" pair

5. 1. Prediction of wear through the energy model

Application of ETW on the example of a «dry» numerical step for one element: let at step n (parameter «Steps» in Ansys Coupled Field Transient): $\tau = 30$ MPa $= 3 \cdot 10^7$ Pa; $v = 0.2$ m/s; $H(T) = 3.5$ GPa $= 3.5 \cdot 10^9$ Pa; $\eta = 0.02$; $\Delta t = 0.5$ s. Then the wear value will be $1.7 \cdot 10^{-5}$ m (purely to demonstrate the order, since in reality η and $H(T)$ should be calibrated)

$$\Delta d = \frac{\eta \tau v \Delta t}{H(T)}. \quad (18)$$

Practical guidelines for processing the Ansys parameter array and additional factors to consider:

– if the initial data does not contain the tangential stress field τ, but the friction coefficient μ and contact pressure p are known, the approximation $\tau \approx \mu p$ can be accepted;

– for fast regimes, it is advisable to take into account the flash temperature T_{flash} – a local instantaneous temperature increase in the microcontact zone of two rough surfaces during sliding. It can be added directly to the *TEMP* field (local instantaneous increase) or implemented through the multiplier $f_T(T)$ in the function $\eta(T,p,v)$;

– triboxidation is taken into account by modifying the solid phase

$$H(T) \to H_{eff}(T,t) = H(T) + H_{oxide} g(T,t), \quad (19)$$

where $H(T)$ – material hardness (temperature dependent), Pa; H_{oxide} – effective hardness or strength of the oxide film formed on the surface under the action of friction and temperature, Pa; $g(T,t)$ – dimensionless function of temperature and time dependence, describing the degree of forma-

tion / destruction of the oxide film (for example, from 0 – no film, to 1 – stable film formed); $H_{eff}(T,t)$ – effective (generalized) surface hardness taking into account the contribution of the film, Pa;

– for contact pairs with partial contact, it is desirable to introduce the contact concentration coefficient $f_c = A_{real} / A_{nom}$, which significantly reduces the effective area and friction energy. The update of the values of the areas A_{real} (real contact area) and A_{nom} (rated contact area) is displayed below during the analysis of the "Status" parameter in Ansys;

– mesh/time convergence of Coupled Field Transient in Ansys by increasing the frequency Δt in the sharp peak phases $q_f = \tau \cdot v$ and checking the effect of the size of the contact elements on $d(x, y)$. To assess mesh convergence or time-step convergence, a comparison of the integrated wear $d(x,y)$ at different contact element densities is usually performed; the relative error should not exceed 5%

$$\varepsilon_d = \left| d_{fine} - d_{coarse} \right| / d_{fine}, \quad (20)$$

where ε_d is the relative error (or convergence) between the calculation results for two grid levels; dfine is the wear depth calculated on a finer (more detailed) grid or with a smaller time step, mm; $|d_{fine} - d_{coarse}|$ is the absolute difference between the results of the two models, mm.

A universal Python postprocessor for Ansys has been developed that reads a data array from a CSV file with contact results (at time points tn / elements) and calculates the local wear depth di according to the given model. The algorithm aggregates the total wear volume V and outputs a wear map by elements (table and plot). The CSV file is exported from Ansys Workbench (Mechanical) with the following columns: time (time, s); element_id (element identifier); area (element area, m^2); tau (tangential stress, Pa). Additionally, the following parameters are passed: p (contact pressure, Pa); v (tangential sliding velocity, m/s); temp (temperature, K); ds (sliding increment (optional, if v is not present), m). For each element, the script calculates the local wear depth according to (12).

So, the postprocessor script for processing the exported CSV file in Python 3.9+ (pandas, numpy, matplotlib are required):

```
import pandas as pd
import numpy as np
import matplotlib.pyplot as plt
# === Material properties functions ===
def H_of_T(T, H0 = 4e9, beta = 1e-3, T0 = 293):
"""Hardness, Pa, accounting for thermal softening.
H(T)=H0*(1 – beta*(T – T0)), clamped to >= 0.
"""
H = H0 * (1.0 – beta * (T – T0))
return np.maximum(H, 1e6) # lower limit (1 MPa)
def eta_func(T, p, v, eta0 = 0.02aT = 1e-4, ap = 0.5, av = 0.01, v0 = 0.1):
"""Wear efficiency (0..1)."""
fT = 1 + aT * (T – 293) # growth with temperature
fp = np.minimum(1.0, ap * (p / H_of_T(T))) # dependence on p/H ratio
fv = 1 + av * np.log(np.maximum(v / v0, 1.0))
return np.clip(eta0 * fT * fp * fv, 0, 1)
# === Data loading ===
df = pd.read_csv("contact_results.csv")
# If ds is present, use it; otherwise, calculate from v * dt
df = df.sort_values(["element_id", "time"])
df["dt"] = df.groupby("element_id")["time"].diff().fillna(0)
# Hardness and η
df["H"] = H_of_T(df["temp"])
df["eta"] = eta_func(df["temp"], df["p"], df["v"])
# Wear increment calculation
if "ds" in df.columns:
df["dd"] = df["eta"] * df["tau"] * df["ds"] / df["H"]
else:
df["dd"] = df["eta"] * df["tau"] * df["v"] * df["dt"] / df["H"]
# Total wear depth per element
wear_depth = df.groupby("element_id")["dd"].sum()
# Wear volume calculation
area = df.groupby("element_id")["area"].first()
V = (wear_depth * area).sum()
print(f"Wear volume calculationy: {V*1e9:.2f} mm³") # in mm³
# === Wear map visualization ===
wear_depth_mm = wear_depth * 1e3 # in mm
wear_depth_mm.plot(kind="bar", figsize=(12,4))
plt.xlabel("Element ID")
plt.ylabel("Wear depth [mm]")
plt.title(«Wear depth distribution by element»)
plt.tight_layout()
plt.show()
```

A practical demonstration of the ETW model application is too cumbersome to cover within the limits of the current scientific paper. It requires a full-fledged transit thermomechanical analysis with spatiotemporal discretization, calibration of temperature-dependent properties $H(T)$, $\eta(T,t)$, as well as integration of results over time steps n in each contact cell (element). The implementation of such an approach involves separate numerical postprocessing with binding to the ANSYS Workbench (Coupled Field Transient) source files, which significantly expands the volume of data and goes beyond the scope of this work. Interest in such an ETW model may primarily be shown by scientific laboratories in electrical materials science based at enterprises manufacturing trolleybus power supply elements (TCI, current collector rods, etc.). ETW can serve as the basis for the construction of so-called "custom" models, which can become the subject of a certain "know-how" and provide a competitive advantage for the manufacturer.

In our study, a simpler previously described energy model of wear (9) was used, which retains the key parameters of the energy approach. Among the latter: the average frictional stress τ_{avg}, the total sliding length s_{total} and hardness H, but without taking into account the temporal change in temperature and local thermomechanical effects. This approach has made it possible to obtain results that are consistent with ETW in terms of physical content – the wear depth d – with significantly lower computational complexity, which is optimal for the initial verification of the energy concept of wear modeling in the "TCI-wire" node.

Thus, the simplified energy model is an effective tool for wear prediction, preceding a much more voluminous and resource-intensive ETW modeling focused on verifying calculations at the final stage (before physical testing of the TCI prototype).

5. 2. Numerical indicators of the stressed state of the "insert-wire" model

A traditional component in any analysis of the stress-strain state (SSS) of a model (including friction problems) is the assessment of the von-Mises Stress. Its purpose is to visually determine the zones of increased stresses σ_{max} and

the nature of their distribution over the body of the model; to compare the obtained values of σ_{max} with σ_y (Yield strength) to determine the zones of possible plastic deformation. Comparative results on TCIs for different materials were obtained (Table 2): the lowest value of $\sigma_{max} = 16.24$ MPa was recorded for Carbon (CY) (Fig. 3, *a*), and the highest (30.53 MPa) was recorded in CU (Fig. 3, *b*), the hardness of which is almost three times higher (Table 1). This is also confirmed visually – the spots of increased stress are intermittent, locally focused (Fig. 3, *b*), and have a much smaller area than in other TCI samples.

The third instance of the EG-TCI demonstrated $\sigma_{max} = 18.99$ MPa (Fig. 3, *c*), which seems to be an optimal intermediate value. However, given the low σ_y threshold, the condition $SF > 1$ (Safety Factor), that is, the safety margin relative to the yield strength of the TCI, was not met. This is evidenced by a large area of red color (plastic deformations) on the SF map (Fig. 4, *a*), where the local peak value $SF = 0.08$.

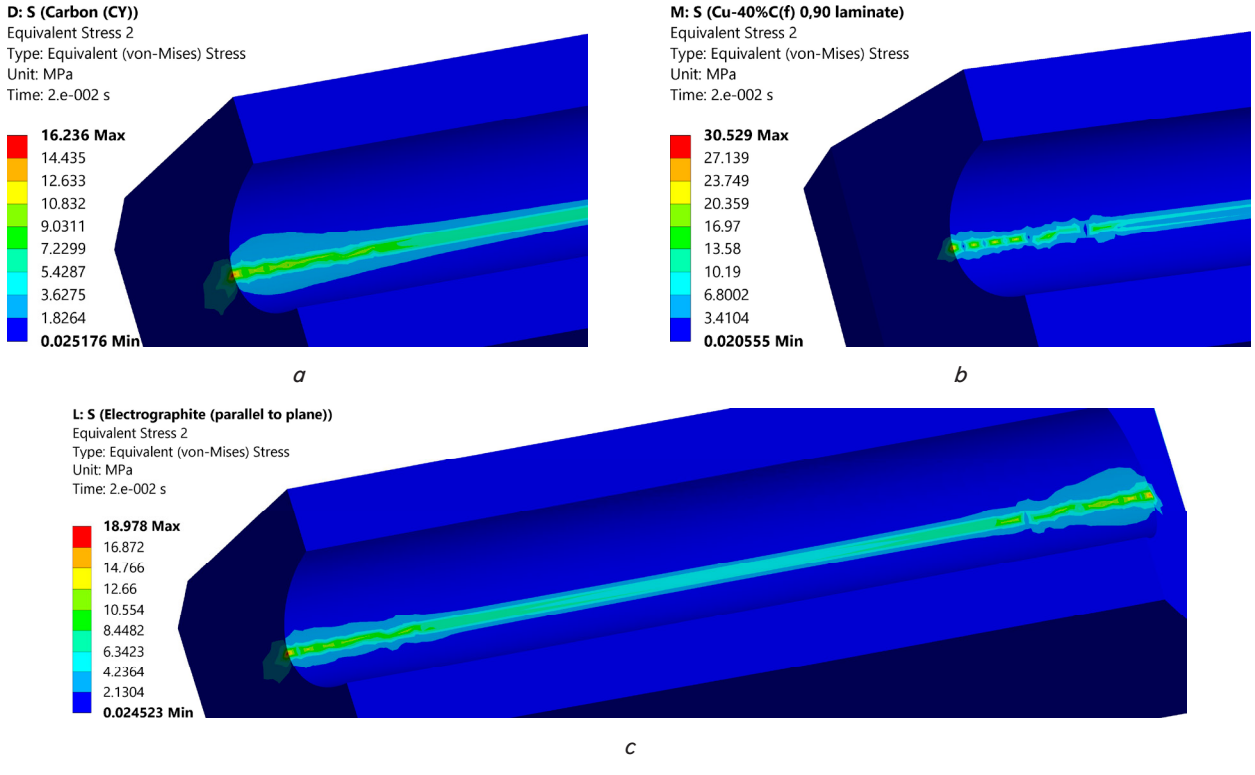

Fig. 3. Von-Mises's stress maps of the insert made of the following materials: *a* – Carbon (CY); *b* – Cu-40% C(f) 0.90; *c* – Electrographite

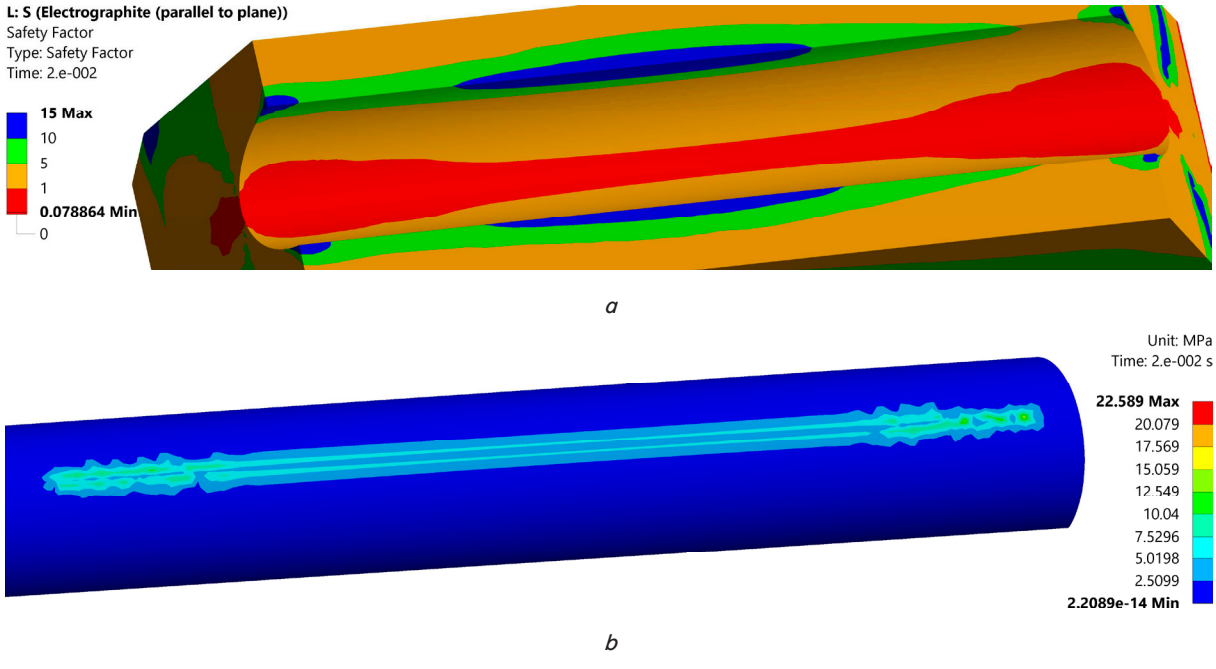

Fig. 4. Stressed-strained state of the models: *a* – Safety Factor of the Electrographite insert; *b* – von-Mises stress of the wire in a pair with the Cu insert – 40% C(f) 0.90

Thus, the increased lubricating ability of this material causes a decrease in the wear resistance of the trolleybus contact insert. This is partly confirmed by the relatively low level of stresses arising in the contact wire for a pair with a TCI of the EG type: $\sigma_{\max} = 15.73$ MPa (Table 2). At the same time, the insert experiences higher contact stresses ($\sigma_{\max} = 18.99$ MPa) than those that it induces on the surface of the wire, which indicates the predominant wear of the insert material. In general, for all considered pairs of "TCI-wire" (Table 2), a pattern is observed according to which the maximum stresses in the insert exceed the corresponding stresses in the wire, which is a necessary condition for the preservation of the contact wire.

However, in the case of TCI EG, the resulting stresses significantly exceed those permissible for SF (Fig. 4, *a*) – $\sigma_y = 1.4$–1.6 MPa (Table 1), which is simultaneously equal to the tensile strength. This literally means that when σ_y is exceeded, the EG TCI immediately begins to wear out.

In a pair with the CU TCI (Fig. 4, *b*), the wire stresses were significantly higher $\sigma_{\max} = 22.59$ MPa. This is the highest value among all samples and was recorded at the very beginning of the contact ($t_{\delta\max} = 0.02$ s) in contrast to other specimens ($t_{\delta\max} = 0.12$ s). The theoretically specified timing (Table 2) indicated the instant stabilization of the contact of the harder CU TCI with the wire surface. This behavior differed from Carbon (CY) and EG, which adhere adhesively and begin to wear out even before the moment of sliding (after 0.12 s), when the stresses drop sharply.

Considering that the energy model (9) is based on τ_{avg} (the average value of Frictional Stress from Ansys – Table 2), the issue of objective measurement of the value of this parameter arises. The values given in Table 2 are averages for the entire surface of the TCI trough (≈ 0.14 MPa for all samples), where most of the contact has a gap (near – yellow areas on the contact status map in Fig. 5, *a*). Only the narrow central strip is characterized by the Sliding contact type. Such an estimation algorithm underestimates the real average value of Frictional Stress and requires localized stress analysis directly in the Sliding region. For this purpose, a separate, much narrower region of the TCI trough, commensurate with the width of the Sliding spot (Fig. 5, *a*), was selected in the Ansys model, and FEA was repeated for both samples (EG and CU). Since the concentration of the measurement area τ_{avg} implied a greater detail of the FEM mesh, the Face Sizing value for the CU TCI was reduced to 0.5 mm (Fig. 5, *b*). An additional reason for such detail is the higher hardness of the CU insert material and, accordingly, a narrower contact spot compared to the EG (Fig. 5, *c*).

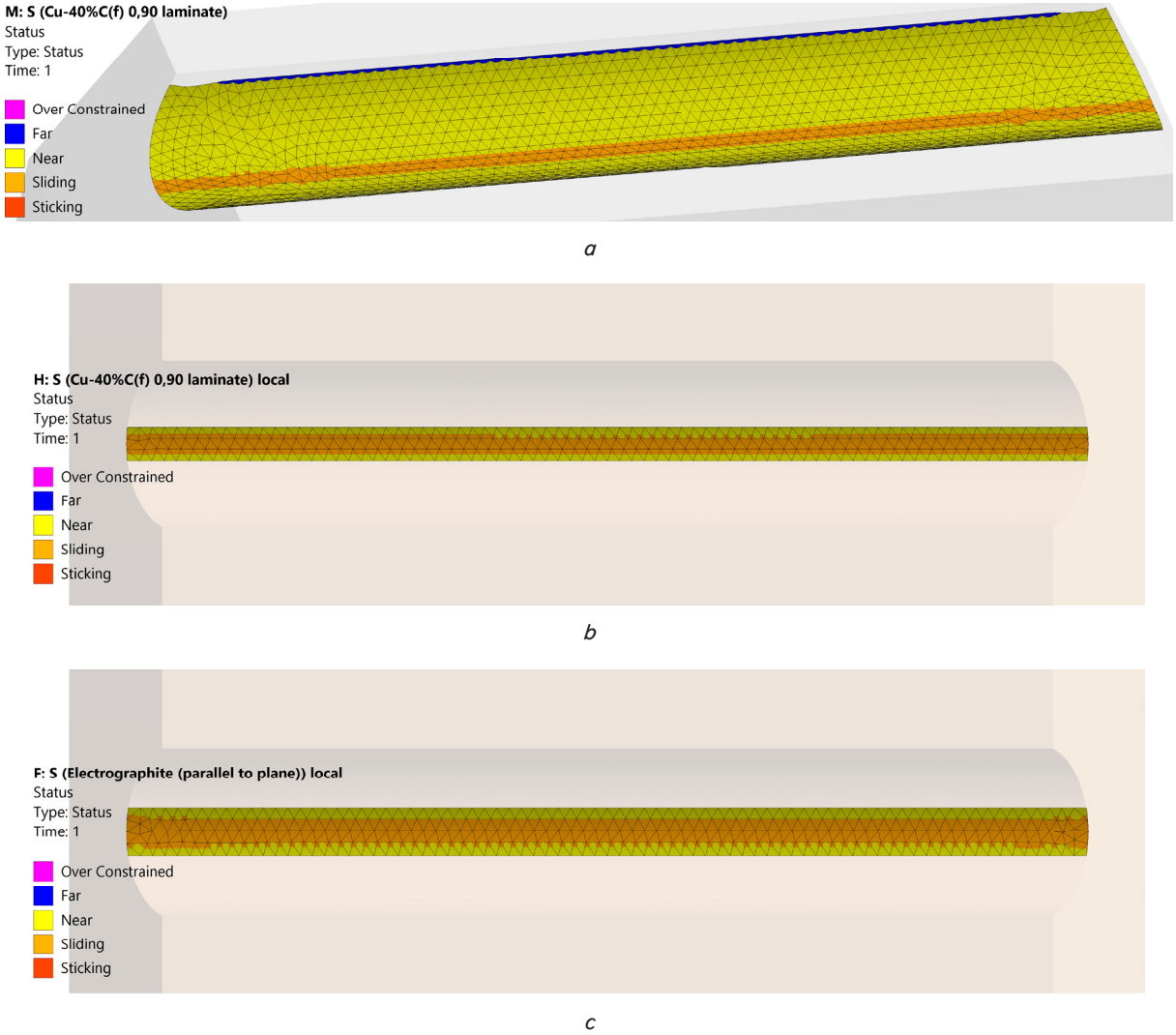

Fig. 5. Status maps of the insert contact: *a* – Cu trough – 40% C(f) 0.90; *b* – Cu localization – 40% C(f) 0.90; *c* – electrographite localization

Results of the average Frictional Stress of the local area of both TCI samples after FEA-recalculation: $\tau_{avg} = 0.439$ MPa for EG and 0.599 MPa for CU, respectively. These values are significantly higher than the previously established (≈0.14 MPa in Table 2) for the full area of the TCI trough. The maximum value of Frictional Stress for TCI CU is $\tau_{max} = 4.42$ MPa (Fig. 6, *a*) at time $t_{\tau max} = 0.72$ s (second half of the experiment). The EG TCI sample showed 3.34 MPa at $t_{\tau max} = 0.007$ (Fig. 6, *b*). This corresponds to the beginning of the experiment and approaches the classical friction model – frictional stress usually reaches its maximum value at the initial stage of sliding. The reason is the static component of friction, when the micro-roughness of the contact surfaces is still interlocked. After overcoming these adhesions, the stress decreases to the level of dynamic friction (at the level of 3.3 MPa for EG), which is more stable. Penetration of the wire into the surface of the EG TCI (red area on the gap map in Fig. 6, *c*) confirmed the completeness of the contact in the designated local zone.

The maximum τ_{max} values of Frictional Stress fluctuated during the movement of TCI along the wire surface and were characterized by different dynamics during the contact period (Fig. 7). The extrema on the plots correspond to the time points in Fig. 6, *a*, *b*.

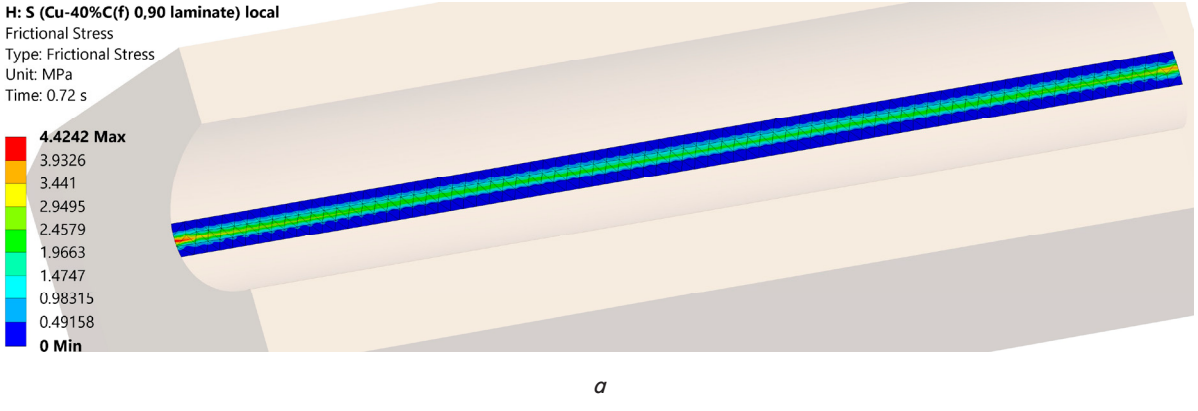

a

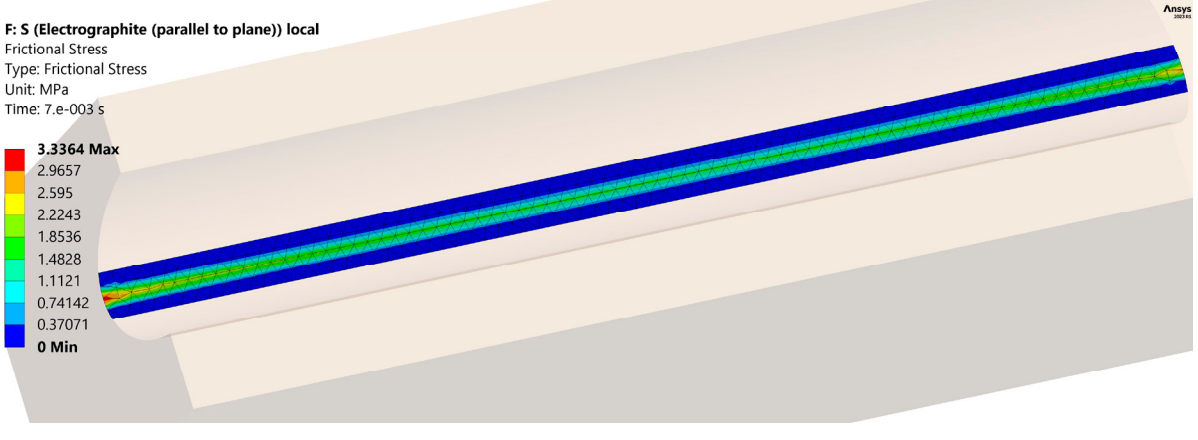

b

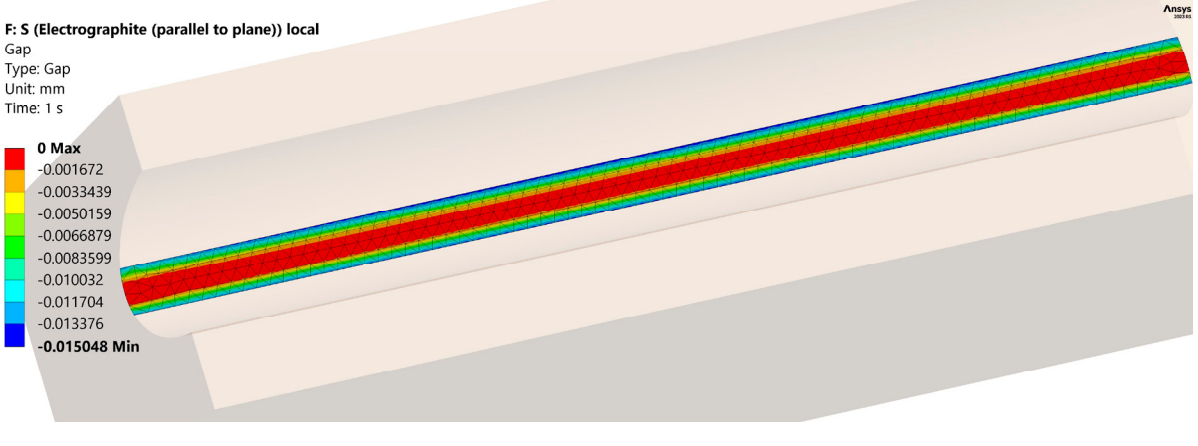

c

Fig. 6. Local analysis of the insert: *a* – frictional stress of the model with Cu-40% C(f) 0.90; *b* – frictional stress of the model with electrographite; *c* – gap of the model with electrographite

Table 2

Von-Mises and frictional stresses in contact pairs "TCI-wire"

Insert material	Insert			Wire	
	δ_{max}, MPa	$t_{\delta max}$, s	τ_{avg}, MPa	δ_{max}, MPa	$t_{\delta max}$, s
Carbon (CY)	16.24	0.02	≳0.138	14.33	0.12
EG	18.99	0.02	≈ 0.139	15.73	0.12
CU	30.53	0.02	≳ 0.140	22.59	0.02

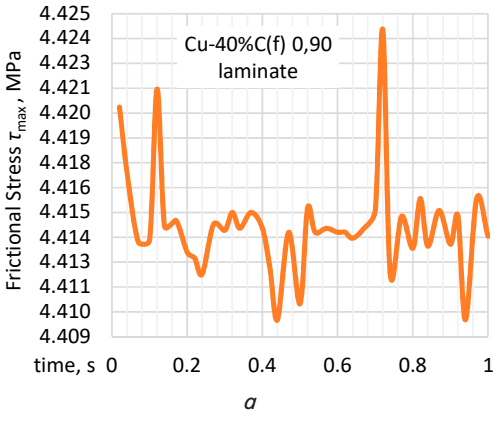

a

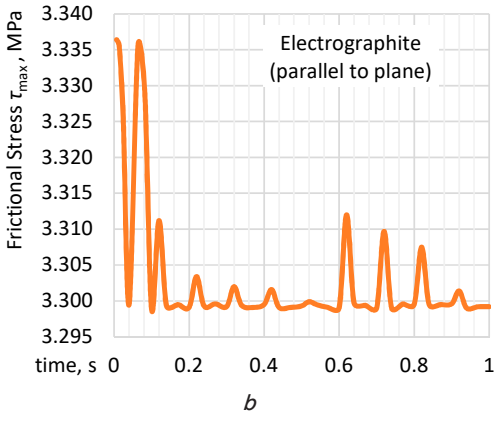

b

Fig. 7. Frictional Stress plots for the insert: *a* – Cu-40% C(f) 0.90; *b* – electrographite

The CY TCI sample was excluded from the localized analysis for a number of reasons (it was initially present in the theoretical analysis). Pure carbon has low impact toughness (especially in amorphous or graphitic forms) – it easily breaks under vibrations and shock pulses (unevenness of the contact network, wire breaks, etc.). Comparison of some of the parameters (according to Ansys Granta EduPack): Fracture toughness (strength against crack propagation) is $(0.8–1.0) \times 10^6$ Pa · $m^{0.5}$ for CY and $(47–55) \times 10^6$ Pa · $m^{0.5}$ for CU; Toughness G (energy crack resistance) is 65–99 and $(14.5–20.0) \times 10^3$ J/m^2, respectively. The next reason is that graphite has significantly lower electrical conductivity than copper or copper-graphite composites. The electrical conductivity for CY is $(200–632) \times 10^3$ Siemens/m, and for CU – $(50–52.4) \times 10^6$ Siemens/m, which corresponds to almost metallic conductivity and approaches that of pure copper. In addition, insufficient lubricity and low stability under humidity and temperature fluctuations are additional stopping factors for the use of CY.

The wear calculation was performed based on the energy model (9) and the obtained results of the average value of Frictional Stress of the local area for samples with EG and CU. It was established that τ_{avg} is 0.439 MPa for EG and 0.599 MPa for CU, respectively. The following parameters of equation (9) were taken as common for both inserts: $\eta = 1 \cdot 10^{-5}$; $S_{total} = 0.2$ m.

Insert with EG: taking into account that the Vickers hardness (Hardness-Vickers) = 4.28–4.72 HV, then the average value $H = 4.5 \cdot 9.81 \cdot 10^6 = 4.41 \cdot 10^7$ Pa or 44.1 MPa. Given Frictional Stress $\tau_{avg} = 0.439$ MPa, $\eta = 1 \cdot 10^{-5}$, $S_{total} = 0.2$ m, then, according to (9), the wear value will be $1.99 \cdot 10^{-5}$ mm. Total extrapolated wear per 100 km or 500 thousand cycles (100000 m / 0.2 m = $5 \cdot 10^5$ cycles)

$$1.99 \cdot 10^{-5} \cdot 5 \cdot 10^5 = 9.95 \text{ mm}.$$

This means that for 450 km, the wear will equal: 9.95 · 4.5 = 47.78 mm, which exceeds the permissible limits.

Note that the technical requirements for TCI state that "the warranty period of operation of the inserts is not less than 450 km in dry weather in the absence of eccentric displacement of the wires at the joints. The depth of the limit wear of the inserts is up to 10 mm". It should be noted that the parameter τ_{avg} was measured under the condition of applying the maximum permissible pressure of the insert on the wire, equal to $p = 0.5$ MPa (Fig. 2, *a*). Under real conditions of trolleybus movement, the pressure value can fluctuate in the range of 0–0.5 MPa, and the contact area can move along the surface of the TCI gutter, which is defined in the UNECE R100 rules. Under the condition of a lower pressure value, for example, 0.25 MPa, the τ_{avg} value was also lower, but not by 50% of those measured above. Simulation of the friction of the full gutter surface (Fig. 5, *a*) with an increase in pressure of 0–0.5 MPa demonstrated the nonlinearity of the Average Status plot (averaged contact status in Ansys) (Fig. 8). The ordinate axis reflects the change in the type of contact between the surfaces, where the value 0 corresponds to the Far mode, 1 = Near mode, and 2 = Sliding mode. Additionally, it should be noted that the contact patch on the surface of the chute migrated during the movement of the trolleybus (turns, inclines, etc.), which distributes the wear over a larger surface, reducing local wear.

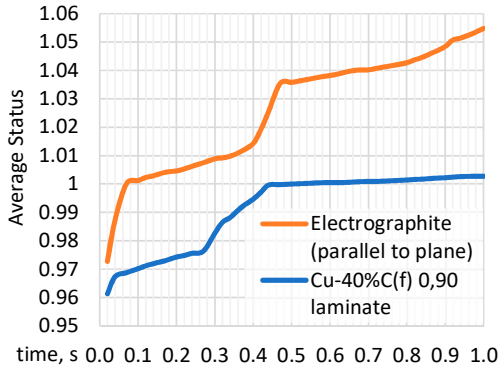

Fig. 8. Average Status plot for insert contact under pressure 0–0.5 MPa

Conclusions on EG: provided that the pressure of the insert on the wire is reduced and the real laboratory value of coefficient η is included in the calculation, EG can theoretically be used in inserts, although the simulation did not confirm the optimality of this variant of the contact pair.

Insert with CU: since the hardness is 120–135 HV, the average value H = $127.5 \cdot 9.81 \cdot 10^6 = 1.25 \cdot 10^9$ Pa or 1250 MPa. Given the average Frictional Stress $\tau_{avg} = 0.599$ MPa, $\eta = 1 \cdot 10^{-5}$ and $S_{total} = 0.2$ m, the wear value according to (9) will be $9.58 \cdot 10^{-7}$ mm. Total wear per 100 km or 500 thousand cycles: $9.58 \cdot 10^{-7} \cdot 5 \cdot 10^5 = 0.479$ mm. For 450 km, the wear will be 2.2 mm, which is within the normal range. At the same time, the hardness value of the CO wire material is lower (Hardness-Vickers 80–115 HV) than the composite insert material. Thus, the wire will wear out first, which is not recommended (its replacement is more expensive than TCI).

6. Discussion of results related to contact interaction in the pair "insert-wire"

Our research results confirm the priority of using CU as the optimal material for TCI: 2.2 mm per 450 km versus 47.78 mm for EG under sliding conditions $S_{total} = 0.2$ m and contact pressure $p = 0.5$ MPa (formula (9), Fig. 7, 8). This difference is explained by the complex thermomechanical nature of wear in the contact pair "TCI-wire", where the local energy balance of friction, temperature-dependent hardness of materials, and spatial distribution of contact stresses play a decisive role (Fig. 3–6, Table 2). Such interaction causes deviations from classical linear dependences of the type HV $\propto \tau$ and determines the real intensity of destruction of the surface layer. In particular, it was found that the maximum Mises stresses in the inserts are $\sigma_{\max} = 16.24$ MPa for CY, 18.99 MPa for EG, and 30.53 MPa for CU, which is directly related to the differences in their hardness and the nature of the contact load distribution (Fig. 3, Table 2). Thus, the results of FEA simulation (Fig. 3–6) in combination with the wear energy model (9) make it possible to directly relate the contact stress distribution to the predicted wear depth of the contact insert.

It has been found that the average value of Frictional Stress *τavg* changes slightly when going from EG to CU (0.439 versus 0.599 MPa) (Table 2), despite the almost 30-fold difference in Vickers hardness (HV) and significant differences in the stress state of the contact pair. These values are significantly higher than those previously established (≈ 0.14 MPa in Table 2) for the full area of the TCI groove. Therefore, the localization of the real sliding zone (Fig. 5, 6) leads to an increase in the calculated τ_{avg} by approximately 3–4 times compared to the averaged value over the entire contact area. This indicates that the simple linear proportionality HV $\propto \tau_{avg}$ is not fulfilled, and the magnitude of the stresses is additionally affected by the material structure, surface roughness, friction coefficient, and other tribological factors.

Our results show that the wear intensity is most sensitive to the contact pressure and friction coefficient, while the influence of the sliding velocity change within the studied range is less pronounced. This is consistent with the used energy model (9), in which the wear depth is directly proportional to τ_{avg} and S_{total} and inversely proportional to hardness *H*. That is why even at close values of τ_{avg} the EG material demonstrates significantly greater wear due to its low hardness, while for CU the higher hardness of 120–135 HV provides a sharp decrease in the depth of fracture of the surface layer. This suggests the existence of materials with a different microstructure, lower roughness, lower friction coefficient, and even higher hardness, capable of providing lower τ_{avg} values in the contact pair "TCI-wire".

The search for such alternatives led to the consideration of the Cu-0.5% Fullerene Soot (FS) composite. FS is representative of a relatively new class of copper-based nanocomposites containing 0.5 wt. % fullerene soot. Fullerene soot, as a by-product of the synthesis of fullerenes (C60, C70, etc.), consists of fullerene-like structures, amorphous carbon, and a small proportion of graphite-like inclusions. This composite is characterized by hardness of about 160 HV; friction coefficient ≈ 0.12; relative density 98.2%; FS particle size 20–40 nm. Maximum hardness is achieved at a content of 0.5% fullerene soot, which provides an optimal balance between strength and wear resistance. Despite the introduction of the carbon phase, the composite retains high thermal conductivity: approximately 288 W/m·K versus 332 W/m·K for pure copper. The electrical conductivity loss is only 10–15% compared to copper, while the wear resistance increases by 40–50%. The low coefficient of friction confirms the high tribological properties.

Given that the hardness of FS exceeds the hardness of CO (≈ 115 HV), this composite is not optimal according to the criterion of priority wear of the insert. At the same time, real wear is determined not only by hardness but also by the friction mechanism, roughness, sliding speed, and oxidation processes. For the "TCI-wire" node, the stability of the oxide film, electrical erosion, contact geometry, and the friction coefficient, which is lower for FS (0.12 versus 0.13), which partially compensates for the difference in hardness, are additionally important.

Under actual conditions, contact wires are usually made not from pure CO copper, but from Cu-Ag, Cu-Sn, Cu-Mg alloys or Cu-ETP (electrolytic tough pitch) copper. In this case, additional hardening to 150–180 HV is carried out by cold deformation, tempering, laser or plasma hardening, ion implantation, or application of hard coatings (TiN, CrN). The base material CO (selected from the Ansys Granta database) was used as a conservative theoretical basis for FEA analysis of the worst-case scenario: when the wire is characterized by significant surface plasticity and low hardness. In other words, if as a result of tribocontact the base CO wire withstands friction with TCI, the modified one will have a higher wear resistance margin, which is extremely positive and will enable the use of EG and CU samples. In this case, the analysis of the data in Table 2 reveals that the maximum stresses in the wire for pairs with CY, EG, and CU are lower than in the corresponding inserts, namely 14.33, 15.73, and 22.59 MPa, which confirms the correctness of the chosen statement of the contact problem and the possibility of a comparative assessment of TCI materials.

Analysis of published studies reveals that most works in the field of trolleybus current collection systems are focused either on macroscopic electromechanical processes or on material characteristics. A comprehensive approach that simultaneously takes into account mechanical, thermal, and energy interaction in the "TCI-wire" node is practically absent. The proposed ETW model combines FEA with an energy-temperature description of wear, takes into account the temperature dependence of hardness, heat flows, and flash temperatures, which makes it possible to reproduce the spatial-temporal distribution of stresses, temperature, and specific friction energy. The transition from contact interaction fields (Fig. 3–6) to temporal and total wear characteristics (Fig. 7, 8) provides a transparent connection be-

tween contact mechanics and quantitative prediction of TCI resource. Thus, the main limitations of classical models that do not take into account thermal effects and local friction energy have been eliminated. It was the integration of the temperature dependence $H(T)$ and the local friction energy that allowed us to quantitatively explain the difference between EG and CU, which did not follow directly from their rated hardness.

Unlike [6–11], in which wear was analyzed mainly on the basis of experimental data or factor analysis without local FEA-distribution of stresses and temperatures, in this study the space-time fields $\tau(x,y,t)$, $p(x,y,t)$ and $T(x,y,t)$ were determined. This made it possible to move from integral estimates to local calculation of the wear depth $d(x,y,t)$ taking into account the real energy balance in the contact zone. It is the space-time fields that determine the local specific friction energy, which within the ETW model acts as a direct driving factor of wear accumulation $d(x,y,t)$, linking mechanical and thermal processes with the real destruction of the surface layer of the material. Compared to an approach from [9], in which the wear prediction was based on generalized empirical dependences without taking into account the temperature-dependent hardness, our results took into account the $H(T)$ function and thermal softening of the material. This ensured a correct transition from the mechanical work of friction to the quantitative assessment of local surface destruction. Unlike studies [13, 14], which mainly considered the material characteristics of nanocomposites without modeling the actual "insert-wire" node, the proposed approach combined the material properties with the boundary conditions formed in accordance with the UNECE standard accelerations. This allowed us to assess the performance of the material not in abstract fashion but under conditions close to operational ones.

In particular, our work has implemented the energy-temperature wear model (ETW) and compared it with the classical Archard and Karman models. Based on the FEA-modeling of the contact interaction of the "TCI-wire" pair, the distribution of contact pressure and frictional stresses was determined, which allowed us to perform a quantitative assessment of the wear of different materials of contact inserts and to substantiate the prospects for the use of copper-fullerene composites.

The main limitation of the work is the use of Granta EduPack reference material data, which do not contain a complete set of parameters for experimental nanocomposites of the FS type. The lack of laboratory characteristics limits the possibility of their full-fledged FEA analysis. At the same time, FS is considered a promising material in the context of transport electrification and the requirements of EURO-7 (Regulation (EU) 2024/1257 – Vehicle emissions and battery durability).

The disadvantage of the study is the lack of experimental verification of the modeling results and the failure to take into account long-term degradation of surface properties. In further research, this could be eliminated by conducting tribological tests, calibrating the ETW model parameters, as well as expanding the material base.

Prospects for research development include optimization of TCI materials based on fullerene-containing composites, multiphysics modeling of the "insert-wire" system together with the energy network, as well as construction of predictive wear models. The main difficulties are the experimental determination of nanomaterial parameters, mathematical identification of temperature dependences, and integration of energy models with full-scale FEA calculations.

7. Conclusions

1. The classical Archard and Karman models adequately describe abrasive-adhesive wear through the relationship between load, hardness, and sliding path, but ignore the influence of temperature, thermal conductivity, and thermal softening of the material. The proposed energy-temperature wear model (ETW) eliminates these limitations by integrating the local heat balance and the dependence of hardness $H(T)$ on temperature. That makes it possible to take into account phase transformations, stress gradients, and sliding speed. At the same time, a physically justified calculation of the wear depth $d(x, y, t)$ is provided in connection with the $\tau(x, y, t)$, $p(x, y, t)$ and $T(x, y, t)$ fields obtained from FEA. Numerical modeling was performed for contact pressure $p = 0.5$ MPa, friction coefficient $\mu = 0.13$, and sliding displacement $S_{total} = 0.2$ m, which corresponds to the characteristic operating conditions of the contact pair "TCI-wire". The ETW model moves from empirical coefficients (e.g., η and μ or α) to energy parameters, which provides a quantitative description of the friction process under dynamic conditions of contact interaction.

2. FEA simulation demonstrated that the contact pair "TCI-wire" under a pressure of 0.5 MPa received frictional stresses $\tau_{avg} = 0.439$ MPa (EG) and 0.599 MPa (CU). The maximum equivalent stresses $\sigma_{\max}$ for the materials were as follows: 16.24 MPa (CY), 18.99 MPa (EG), and 30.53 MPa (CU). At the same time, lower maximum stresses were recorded in the contact wire: 14.33 MPa (CY), 15.73 MPa (EG), and 22.59 MPa (CU), which confirms the fulfillment of the condition of priority wear of the insert compared to the wire. The maximum stresses in the wire occurred at different contact times: $t_{\delta\max} \approx 0.12$ s for CY and EG and $t_{\delta\max} \approx 0.02$ s for CU, which indicates faster stabilization of the contact for the harder CU composite. It was determined that the EG electrographite does not withstand the $SF > 1$ condition at sliding $S_{total} = 0.2$ m due to the low yield strength (1.4–1.6 MPa), which leads to intensive wear – up to 47.78 mm at 450 km (higher than the normatively permissible 10 mm). The copper-graphite CU composite provides several times lower wear intensity (2.2 mm at a distance of 450 km) due to a harder matrix (120–135 HV), uniform distribution of contact stresses, and stable sliding mode without peak overloads. At the same time, when selecting TCI materials, it is necessary to control the condition of priority of wear of the insert compared to the wire, which is a guarantee of preserving the integrity of the city electric power supply network for trolleybuses.

Based on a comparison of copper and graphite composites, the feasibility of using the Cu-0.5% FS material, which combines the high electrical conductivity of copper ($\approx 5 \cdot 10^7$ S/m) with nanoreinforcement with fullerene particles, was substantiated. Due to the formation of a bimodal grain structure, the hardness increases to 160 HV, and the heat resistance – to 700°C, which is 1.3–1.5 times higher than the indicators of the classical copper-graphite composite. Fullerenes act as a nanolubricating phase, reducing the friction coefficient to 0.12 and the wear intensity

by 2–2.5 times. Such properties make FS a promising material for new-generation TCIs, capable of providing stable current collection, lower heat losses, and a significantly longer operating life at elevated temperatures and loads.

Conflicts of interest

The authors declare that they have no conflicts of interest in relation to the current study, including financial, personal, authorship, or any other, that could affect the study and the results reported in this paper.

Funding

The study was conducted without financial support.

Data availability

All data are available in the main text of the manuscript.

Use of artificial intelligence

The artificial intelligence tool ChatGPT (OpenAI, GPT-5 series model) was used to edit the manuscript, increase clarity of presentation, and improve stylistic consistency. The use of this tool did not affect the formation of the scientific content of the work, the analysis of experimental and numerical data, the interpretation of the obtained results, or the formulation of conclusions. All methodological approaches, analytical procedures, and final scientific generalizations were carried out by the authors who bear full responsibility for the content of the submitted manuscript.

Authors' contributions

Kostyantyn Holenko: Conceptualization, Methodology, Writing – original draft; **Oleksandr Dykha**: Methodology, Validation, Writing – review & editing, Supervision; **Orest Horbay**: Validation, Formal analysis; **Oleksii Kovtun**: Formal analysis, Supervision; **Volodymyr Dytyniuk**: Investigation, Visualization.

References

1. Wilk, A., Bartłomiejczyk, M., Skibicki, J., Jarzębowicz, L., Karkosinski, D. R., Hupka, Ł. et al. (2025). Processing and analysis of trolleybus traction data using LINQ technology. Bulletin of the Polish Academy of Sciences Technical Sciences, 73 (4), 154144–154144. https://doi.org/10.24425/bpasts.2025.154144
2. Jakubowski, A., Jarzebowicz, L., Bartłomiejczyk, M., Skibicki, J., Judek, S., Wilk, A., Płonka, M. (2021). Modeling of Electrified Transportation Systems Featuring Multiple Vehicles and Complex Power Supply Layout. Energies, 14 (24), 8196. https://doi.org/10.3390/en14248196
3. Apostolidou, N., Papanikolaou, N. (2018). Energy Saving Estimation of Athens Trolleybuses Considering Regenerative Braking and Improved Control Scheme. Resources, 7 (3), 43. https://doi.org/10.3390/resources7030043
4. Barbone, R., Mandrioli, R., Ricco, M., Paternost, R. F. P., Franco, F. L., Grandi, G. (2022). Flexible and Modular Model for Smart Trolleybus Grids. 2022 IEEE 16th International Conference on Compatibility, Power Electronics, and Power Engineering (CPE-POWERENG), 1–6. https://doi.org/10.1109/cpe-powereng54966.2022.9880904
5. Paternost, R. F., Mandrioli, R., Barbone, R., Ricco, M., Cirimele, V., Grandi, G. (2022). Catenary-Powered Electric Traction Network Modeling: A Data-Driven Analysis for Trolleybus System Simulation. World Electric Vehicle Journal, 13 (9), 169. https://doi.org/10.3390/wevj13090169
6. Skurikhin, V. (2014). Determination of wearproofness of contact wire by the method of complete factor experiment. Technology Audit and Production Reserves, 1 (2 (15)), 26–30. https://doi.org/10.15587/2312-8372.2014.21251
7. Bolshakov, Yu. L., Antonov, A. V. (2015). Investigation of properties of current collector elements and their effect on the performance of tribosystem «contact wire - current collector element». Science and Transport Progress, 6 (60), 35–44. https://doi.org/10.15802/stp2015/57006
8. Chen, M., Allen, T. (2021). Trolleybus Catenary-Pantograph Self-generation Contact Force Under Preload. World Journal of Applied Physics, 6 (4), 60. https://doi.org/10.11648/j.wjap.20210604.12
9. Dykha, A., Aulin, V., Makovkin, O., Posonskiy, S. (2017). Determining the characteristics of viscous friction in the sliding supports using the method of pendulum. Eastern-European Journal of Enterprise Technologies, 3 (7 (87)), 4–10. https://doi.org/10.15587/1729-4061.2017.99823
10. Pan, L., Yang, C., Xing, T., Yu, Q. (2025). An Experimental Investigation of the Electrical Tribological Characteristics of a Copper–Silver Alloy Contact Wire/Novel Pure Carbon Slider. Lubricants, 13 (2), 87. https://doi.org/10.3390/lubricants13020087
11. Chen, T., Song, C., Liu, Z., Wang, L., Hou, X., Lu, H., Zhang, Y. (2023). Current-carrying tribological properties of an elastic roll ring under different currents. Wear, 514-515, 204590. https://doi.org/10.1016/j.wear.2022.204590
12. Holenko, K., Dykha, O., Koda, E., Kernytskyy, I., Horbay, O. et al. (2025). Peculiarities of Assessing Body Strength When Converting a Bus from Diesel to Electric Traction Following the UNECE R100 Regulation. Applied Sciences, 15 (14), 8115. https://doi.org/10.3390/app15148115
13. Cao, Z., Li, R., Shou, M., Luo, R., Wei, B., Wang, T. (2024). Mechanical properties and tribological behaviors of Ag/graphene composite coating under sliding friction and current-carrying fretting. Tribology International, 197, 109811. https://doi.org/10.1016/j.triboint.2024.109811

14. Li, S., Yang, X., Kang, Y., Li, Z., Li, H. (2022). Progress on Current-Carry Friction and Wear: An Overview from Measurements to Mechanism. Coatings, 12 (9), 1345. https://doi.org/10.3390/coatings12091345
15. Ogasawara, T., Ishida, Y., Kasai, T. (2009). Mechanical properties of carbon fiber/fullerene-dispersed epoxy composites. Composites Science and Technology, 69 (11-12), 2002–2007. https://doi.org/10.1016/j.compscitech.2009.05.003
16. Kubo, S., Tsuchiya, H. (2005). Wear Properties of Metal-Impregnated Carbon Fiber-Reinforced Carbon Composite Sliding Against a Copper Plate Under an Electric Current. World Tribology Congress III, Volume 1, 85–86. https://doi.org/10.1115/wtc2005-63457
17. Zhu, W., Miser, D. E., Geoffrey Chan, W., Hajaligol, M. R. (2004). Characterization of combustion fullerene soot, C60, and mixed fullerene. Carbon, 42 (8-9), 1463–1471. https://doi.org/10.1016/j.carbon.2004.01.076
18. Bucca, G., Collina, A. (2009). A procedure for the wear prediction of collector strip and contact wire in pantograph–catenary system. Wear, 266 (1-2), 46–59. https://doi.org/10.1016/j.wear.2008.05.006
19. P., A. K., V., V. N., Joshi, G., Mehta, K. P. (2021). Fabrication and applications of fullerene-based metal nanocomposites: A review. Journal of Materials Research, 36 (1), 114–128. https://doi.org/10.1557/s43578-020-00094-1
20. Zhao, H., Barber, G. C., Liu, J. (2001). Friction and wear in high speed sliding with and without electrical current. Wear, 249 (5-6), 409–414. https://doi.org/10.1016/s0043-1648(01)00545-2
21. Fals, A. E., Hadjiev, V. G., Robles Hernández, F. C. (2012). Multi-functional fullerene soot/alumina composites with improved toughness and electrical conductivity. Materials Science and Engineering: A, 558, 13–20. https://doi.org/10.1016/j.msea.2012.07.027
22. Dub, S. N., Haftaoglu, C., Kindrachuk, V. M. (2021). Estimate of theoretical shear strength of C60 single crystal by nanoindentation. Journal of Materials Science, 56 (18), 10905–10914. https://doi.org/10.1007/s10853-021-05991-2
23. Holenko, K., Dykha, A., Dytyniuk, V., Dykha, M., Horbay, O. (2025). Simulation of the Shaft Surface Strengthening as a Result of Discrete Electro-Mechanical Processing. Advanced Manufacturing Processes VI, 525–534. https://doi.org/10.1007/978-3-031-82746-4_46
24. Dykha, A. V., Zaspa, Yu. P., Slashchuk, V. O. (2018). Triboacoustic Control of Fretting. Journal of Friction and Wear, 39 (2), 169–172. https://doi.org/10.3103/s1068366618020046